

RESEARCH

Open Access



A novel approach utilizing spirocyclic thiopyrimidinone compounds against herpes simplex virus with underlying antiviral mechanisms of action

Esraa A. Manie^{1*}, Emad M. Elzayat^{2*}, Sherif S. Ragab³, Ayman M. Sweed⁴, Hosny Ibrahim⁵, Sherif Nasser⁶ and Abdou K. Allayeh⁷

Abstract

In recent decades, viral outbreaks have significantly threatened global health, with herpes simplex virus type 2 (HSV-2) being one of the most prevalent infections. This study evaluated novel spiropyrimidine derivatives as potential antiviral agents against HSV-2, building on previous research that examined spirocyclic thiopyrimidinone derivatives against human coronavirus 229E (hCoV-229E). Among the eleven synthesized compounds, spiropyrimidinone derivative **3** demonstrated promising antiviral activity, with a selectivity index of 11.2. The drug mechanism of infection studies indicated that compound **3** primarily inhibits HSV-2 at the viral adsorption stage, achieving approximately 83% inhibition and reducing viral multiplication by 34%. Its efficacy is linked to its diketone moiety, which is known for its ability to enhance antiviral effects. Furthermore, the effect of compound **3** on viral inhibition is reflected in the level of caspase-3 protein expression, revealing that the apoptotic pathway is modulated. Docking studies revealed multiple interactions with herpes virus entry mediator (HVEM), indicating its potential as an entry inhibitor. These findings confirm that compound **3** could be a potential candidate for further development in HSV-2 antiviral therapy.

Keywords Antiviral activity, Mechanism of action, Spirocyclic thiopyrimidinones, Herpes simplex virus

Introduction

In the past few decades, humanity has faced numerous large-scale outbreaks of viral diseases that have posed significant threats to human life and well-being. Examples of such outbreaks include COVID-19, avian influenza, Zika virus, and Monkeypox, among other various viral infections that affect humans. Herpes simplex virus stands out as one of the most prevalent, with over two-thirds of the global population being infected [1]. The World Health Organization (WHO) reported that herpes simplex virus type 2 (HSV-2), which is transmitted primarily through sexual contact, affects approximately

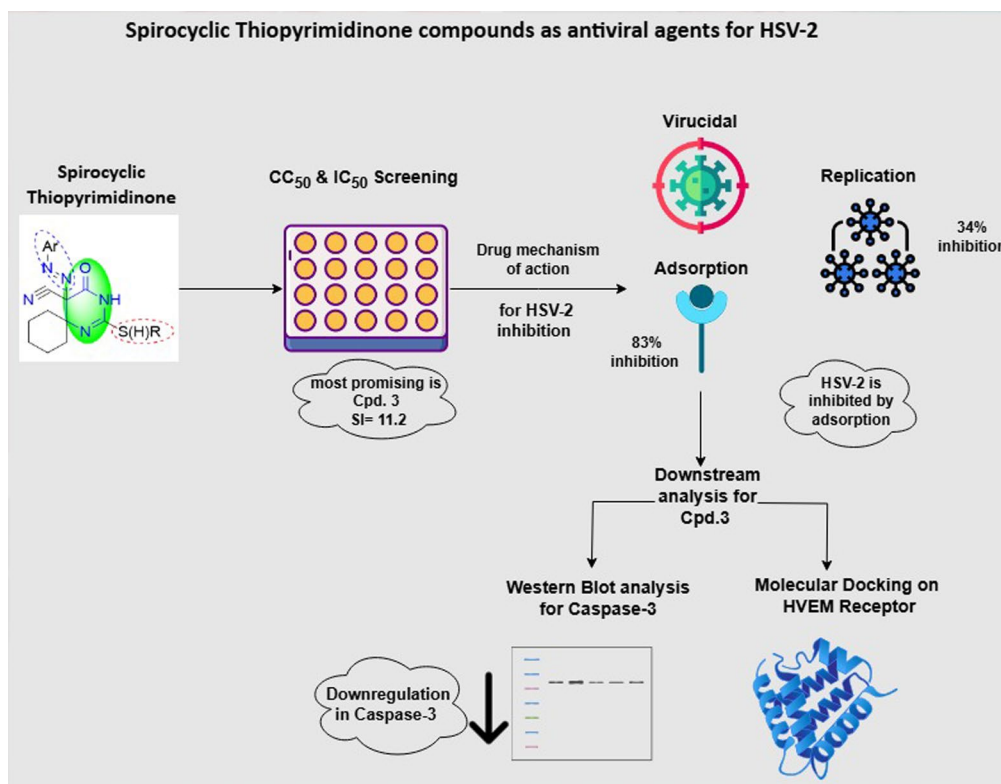
*Correspondence:

Esraa A. Manie
esraamanie125@gmail.com
Emad M. Elzayat
elzayat@sci.cu.edu.eg

Full list of author information is available at the end of the article



© The Author(s) 2025. **Open Access** This article is licensed under a Creative Commons Attribution 4.0 International License, which permits use, sharing, adaptation, distribution and reproduction in any medium or format, as long as you give appropriate credit to the original author(s) and the source, provide a link to the Creative Commons licence, and indicate if changes were made. The images or other third party material in this article are included in the article's Creative Commons licence, unless indicated otherwise in a credit line to the material. If material is not included in the article's Creative Commons licence and your intended use is not permitted by statutory regulation or exceeds the permitted use, you will need to obtain permission directly from the copyright holder. To view a copy of this licence, visit <http://creativecommons.org/licenses/by/4.0/>.

Graphical Abstract

500 million individuals worldwide between the ages of 15 and 49. Each year, there are approximately 20 million new cases of HSV-2, surpassing the number of new cases of other sexually transmitted diseases (STDs) or the number of sexual partners. Notably, the prevalence of HSV-2 is particularly high in sub-Saharan Africa, reaching 70%. This high prevalence in the region may contribute to the transmission and spread of HIV-1 [2].

Herpes simplex virus type 2 is a double-stranded DNA virus enveloped with a multitude of glycoproteins on its surface. These glycoproteins play crucial roles in viral propagation and are subject to cleavage by proteases, highlighting the intricate interplay between different viral components. HSV-2 belongs to the Herpesviridae family, specifically the Alphaherpesvirinae subfamily, which includes eight human viruses capable of causing chronic infections and psychological distress [3]. Following the initial infection, herpes viruses establish latency within the sensory neural ganglia, typically the sacral ganglion, in the case of HSV-2 infection [4]. HSV infections are pervasive and can manifest in various forms, ranging from localized mucocutaneous lesions to disseminated infections affecting individuals of all age groups. Neonatal herpes simplex virus disease, in particular, carries a high risk of morbidity and mortality [5]. Widespread

HSV-2 infection can lead to painful blisters or ulcers that commonly affect the skin, mouth, lips, eyes, and genitals, leading to a range of diseases, such as encephalitis, meningitis, cold sores, genital herpes, and herpes stromal keratitis. Unfortunately, no vaccines are currently available for the prevention of HSV-2 infection [6].

The effectiveness of current antiviral drugs against HSV-2 is limited by their potency and the potential for adverse side effects. These drugs can be classified into two categories: nucleoside inhibitors and nonnucleoside inhibitors. Examples of nucleoside inhibitors include acyclovir, penciclovir, ganciclovir, famciclovir, and valacyclovir. Nonnucleoside inhibitors include foscarnet, cidofovir, and docosanol [7]. However, the emergence of drug-resistant strains of the virus has highlighted the urgent need for more efficient treatment options. To address this challenge, researchers have developed a diverse range of pyrimidine-based antiherpes drugs, some of which are already approved and available on the market (Fig. 1).

Structurally, acyclovir, ganciclovir, valacyclovir, and penciclovir share a common aminopurine scaffold, specifically the imidazopyrimidine moiety, but with different substituents at the 9-position. These compounds are nucleoside analogs and are among the most commonly used drugs for HSV-2 treatment. On the other hand,

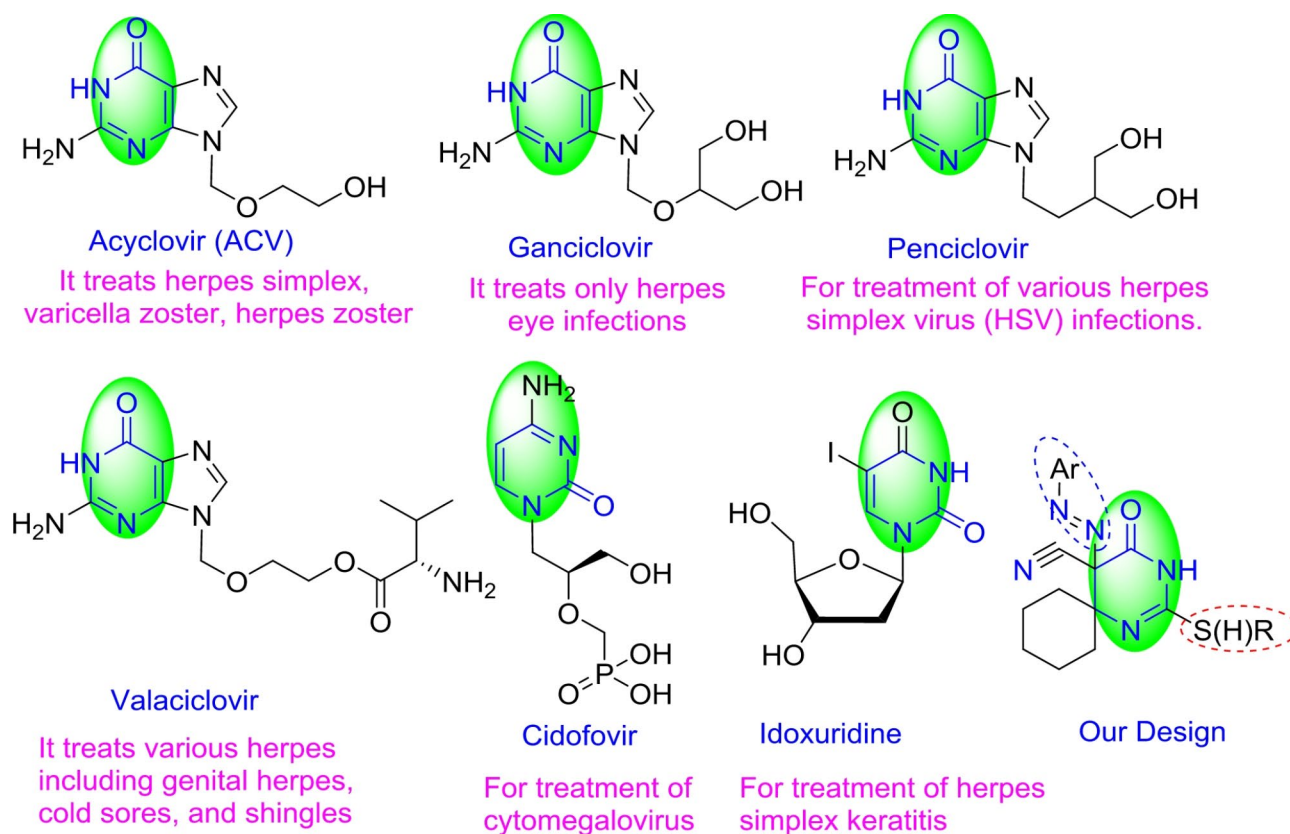


Fig. 1 Antiherpes drugs containing pyrimidine moieties

cidofovir is an acyclic monophosphate nucleotide analog with an aminopyrimidinone fragment. Idoxuridine, on the other hand, is a nucleoside analog with an iodopyrimidinone moiety resulting from the modification of deoxyuridine [8]. In continuation of the efforts dedicated to the development of antiherpes drugs, we synthesized new nonnucleoside siprothiopyrimidine derivatives to investigate their antiherpes activities.

Materials and methods

Preparation of the compounds, cells and virus

All synthetic compounds were prepared according to the methods of Ragab et al. [9] and dissolved in dimethyl sulfoxide (DMSO) to prepare a 100 mg/ml stock, and adherent African green monkey kidney cells (Vero) were cultured in Dulbecco's modified Eagle's medium (DMEM) supplemented with 10% fetal bovine serum (FBS) and a 1% antibiotic penicillin/streptomycin mixture. The human herpes simplex virus type 2 was kindly provided by Nawah-Scientific Centre, Egypt.

Statistical analysis: The data were analyzed via GraphPad Prism analysis software version 5 for Windows (developed by GraphPad Software, Inc., USA). The data were analyzed via Student's *t*-test and ANOVA (analysis of variants) via the SPSS statistical software package version 20. The data are expressed as the means and

standard deviations (SDs). $p < 0.05$ was considered to indicate statistical significance.

Screening for cytotoxicity via a crystal Violet assay

A volume of 100 μ L of cell suspension containing 10^4 cells was placed in each well of a 96-well plate. The plates containing the cells were then placed in a 5% humidified CO_2 incubator at 37 $^\circ\text{C}$ for 24 h to allow the cells to form a confluent monolayer. By twofold serial dilution, each compound was diluted in 0.01 mL of medium, starting with a concentration of 1000 $\mu\text{g}/\text{mL}$. The diluted compounds were then cultured for 72 h at 37 $^\circ\text{C}$ in an environment with 5% CO_2 . Each concentration was tested 3 times. After the incubation period, the supernatant was discarded, and the cells were washed with 1x phosphate-buffered saline (PBS). The cells were then fixed with 100 μ L of 10% formaldehyde and incubated at room temperature for 20 min. The cells were subsequently washed five times with running water. Next, 50 μ L of a 0.1% solution of crystal violet dye (LOBA CHEMIE. LTD; C.I.No. 42555) was added to each well and incubated for 15 min. The cell monolayers were washed again and allowed to air dry. Finally, the crystal violet dye was dissolved by adding 200 μ L of methanol, and the mixture was incubated for 20 min. The absorbance was measured via an ELISA plate reader (FLUOstar Omega Ω) at a wavelength of 570 nm

[10]. Cell viability was calculated as a percentage of the average optical density of the cell controls, which was set to 100%. The 50% cytotoxic concentration (CC_{50}) was calculated via mean dose-response curves via GraphPad Prism.

Screening the antiviral activity by MTT

In accordance with the previous section, the CC_{50} (50% cytotoxic concentration) of each compound was determined as the starting point for screening its antiviral activity. A volume of 100 μ L of cell suspension containing 10^4 cells was added to each well of a 96-well plate. The plates with the cells were then placed in a 5% humidified CO_2 incubator at 37 °C for 24 h to allow the cells to adhere and form a monolayer. The cell monolayers were subsequently washed once with 1x phosphate-buffered saline (PBS) and infected with herpes simplex virus type 2 (HSV-2) (MOI = 1) in triplicate for 1 h. After the infection period, 100 μ L of each compound's serial dilution was added to the infected cells. A triplicate of untreated infected cells was included as a positive control (VC), and the mixture was incubated for 72 h at 37 °C in a 5% CO_2 incubator. Following the 72-hour incubation, the supernatant medium was removed, and the cell monolayers were washed with 1x PBS. Then, 25 μ L of a 0.5 mg/mL solution of MTT (3-(4,5-dimethylthiazol-2-yl)-2,5-diphenyltetrazolium bromide) obtained from Sigma-Aldrich, Saint Louis, MO, USA, was added to each well and incubated for 2 h at 37 °C. The MTT reagent was subsequently discarded, and 200 μ L of acidified isopropanol (1 N HCl in 99.9% isopropanol) was added to dissolve the formazan crystals formed by the viable cells. Finally, the color intensity was measured, and the absorbance was recorded via an ELISA plate reader. The data obtained were used to calculate the IC_{50} values (50% inhibitory concentration) via nonlinear regression analysis. This was accomplished by plotting the logarithm of the inhibitor concentration against the normalized response. The analysis was performed via GraphPad Prism 5 analysis software [11, 12].

Identifying the Inhibition mechanisms of action

To gain a better understanding of how each compound's antiviral activity inhibits specific steps in the viral cycle, we investigated three mechanisms: virus adsorption, virus replication, and viral fusion (virucidal). For the adsorption mechanism, we seeded 100 μ L of cell suspension into 96-well cell culture plates under the previously mentioned conditions. After 24 h, the medium was discarded, and the adherent cells were washed with 1x PBS. Then, we added 100 μ L of each promising compound at a pretested safe cytotoxic concentration (CC_{50}) to the cells in triplicate. The plates were then incubated at 4 °C for 1 h to allow the compounds to adsorb onto the cell

receptors. After incubation, the compound was removed, and the cells were washed again with 1x PBS. Next, we added 100 μ L of the virus mixture (MOI = 1) to each well and incubated it for 1 h at 37 °C in a CO_2 incubator. The virus was removed, and the cells were washed once more with 1x PBS. Finally, we added 100 μ L of maintenance media containing 3% bovine serum albumin (BSA) and incubated the plates for 72 h at 37 °C in a 5% CO_2 incubator. For the replication mechanism, we added 100 μ L of diluted virus (MOI = 1) to a preseeded 96-well cell culture plate and incubated it for 1 h at 37 °C in a CO_2 incubator. After incubation, the virus was removed, and 100 μ L of each compound was added in triplicate. The plates were then incubated for 1 h at 37 °C in a CO_2 incubator. Next, 100 μ L of maintenance medium was added to each well. For the virucidal mechanism, we mixed an equal volume of the safe concentration of the pretested compound with the virus dilution (MOI = 1) and incubated the mixture at room temperature for 1 h. We subsequently prepared twofold serial dilutions of the mixture and inoculated them into the cells, which were then incubated for 1 h at 37 °C in a CO_2 incubator. After incubation, the supernatant was removed, the cells were washed, and 100 μ L of maintenance media was added. The plates were then incubated for 72 h at 37 °C in a 5% CO_2 incubator. Following the incubation periods, we removed the medium and washed the cell monolayer with 1x phosphate-buffered saline (PBS). Next, we added 25 μ L of 0.5 mg/mL MTT (3-(4,5-dimethylthiazol-2-yl)-2,5-diphenyltetrazolium bromide, Sigma-Aldrich, Saint Louis, MO, USA) and incubated the plates for 2 h at 37 °C. After incubation, the MTT reagent was discarded, and 200 μ L of acidified isopropanol (1 N HCl in 99.9% isopropanol) was added to dissolve the formazan crystals that had formed. Finally, we measured the absorbance at $\lambda = 570$ nm via a plate reader (FLUOstar Omega Ω) [11, 12].

Western blotting

A 3 ml cell suspension was cultured in six-well cell culture plates supplemented with complete DMEM and then incubated at 37 °C in a 5% CO_2 incubator for 24 h. After incubation, the supernatant was discarded, and the cell monolayer was washed with 3 ml of 1x PBS. The cell monolayer was then treated in duplicate according to the IC_{50} . Duplicates for cell and virus control were included. The cell pellets were collected at 1, 3, 6, 12, and 24 h postinfection. The cell pellets were lysed with ice-cold RIPA lysis buffer supplemented with fresh protease inhibitor cocktail, incubated for 30 min on ice, and centrifuged at 15,000 RPM at 4 °C for 20 min, after which the supernatant was transferred to a fresh tube. The total water-soluble protein concentration was quantified via a bicinchoninic acid protein assay kit (Micro BCA™ Protein Assay Kit, REF: 23235; Thermo Scientific). Ten

micrograms of protein were loaded in 2x Laemmli buffer and separated via 12% sodium dodecyl sulfate–polyacrylamide gel electrophoresis (SDS–PAGE) along with a protein ladder (Cat. No. PM008-0500, GeneDirex, Taiwan). The proteins were transferred to a 0.2 μm PVDF membrane (REF.03010040001, Sigma Aldrich, St. Louis, MO, USA) by a Mini-PROTEAN® Tetra Cell and Mini Trans-Blot (Bio-Rad) in transfer buffer (Bio-Rad Tris/Glycine transfer buffer Cat. #1610734) for 45 min at 100 V and 350 mA. β -actin (REF. No. MA5-11869; Invitrogen) was detected as a housekeeping protein against the Caspase-3 mAb (REF. No. 9662 S, Cell Signaling, Danvers, MA, USA) at a 1:1000 dilution via horseradish peroxidase-conjugated anti-mouse IgG (61-6520; Invitrogen) and anti-rabbit IgG (31460; Invitrogen) diluted 1:3000. Bands were detected via SuperSignal™ West Pico PLUS Chemiluminescent Substrate enhanced chemiluminescence (ECL, REF. 34577, Thermo Scientific, USA). Images were captured with a Bio-Rad ChemiDoc gel documentation imaging system and analyzed by Image Lab (Bio-Rad 6.1) [13].

Molecular Docking

The crystal structure of the herpes simplex virus glycoprotein bound to the HVEM receptor (PDB ID: 1JMA) was retrieved from the RCSB Protein Data Bank [14]. To prepare the protein, it was imported into the PDB Reader and Manipulator module in CHARMMGUI. Initially, only chain A, which corresponds to the HVEM receptor, was retained for further processing. Missing hydrogen atoms were added, and the system's pH was adjusted to 7.4 to ensure accurate protonation states of the residues. Additionally, residues 93 and 94 were modeled to address any gaps. The resulting. pdb file was then imported into Chimera, where partial charges were assigned via the AMBER ff14SB force field [15–18]. The modified protein structure was subsequently analyzed via fpocket and CASTp to identify potential binding sites [19]. CASTp identified a binding site involving residues Gln59, Cys81, Gly94, His96, and Cys97, which was ranked second, with a surface area of 15.855 \AA^2 and a volume of 8.815 \AA^3 . Similarly, the pocket also ranked second, with a pocket score of 24.7220, including residues Tyr45, Gln59, Thr76, Glu77, Asn78, Ala79, Val80, Cys81, Gly94, His96, and Cys97. Notably, the highest-ranked binding sites differed between the two methods, leading to the selection of this second-best site as the preferred binding site [20, 21].

The tested compounds (2, 3, and 5c) were drawn using ChemBioDraw Ultra. They were prepared by adding hydrogen atoms at pH 7, calculating partial charges via AM1-BCC, and performing energy minimization to the nearest local minimum via 1000 steps with the steepest descent algorithm in Chimera. The protein was then imported into GOLD software, where a cavity file was

created to specify the residues comprising the binding site. The compounds were loaded into GOLD, generating 50 GA solutions for each compound, with ChemPLP as the scoring function. The resulting poses were clustered using a threshold of 1.5 \AA with the complete linkage method. The best-ranked pose from the most populated cluster was saved as a ligand–protein complex, which was then uploaded to the Protein–Ligand Interaction Profiler (PLIP) and visualized via PyMOL [22–23].

Results

The cytotoxicity and antiviral activity of the compounds

Recently, the synthesis of highly bioactive azo dye derivatives by the diazocoupling of aryl diazonium compounds with spirocyclic thiouracil and their antiviral activity against RNA viruses were evaluated [9, 24]. These compounds were prepared according to the authors' previous protocol from the starting precursor 1 using three alkylating agents: methyl iodide, α -chloroacetylacetone, and α -chloroacetoacetanilide (Fig. 2). Two series of azo dye derivatives, 5a-f and 6a-c were generated through the diazotization of the two starting precursors, spirothiopyrimidinones 1 and 4, respectively, under basic conditions in satisfactory yields. Spirothiopyrimidinone 1 contains one active methine proton at the 5-position of the pyrimidinone nucleus, whereas the other derivative, 4, contains an additional active methine proton on the diketone fragment. The aryl diazonium salts were directed mainly toward the methine center of compound 4, which is in close proximity to the nitrile and carbonyl groups of the pyrimidinone nucleus. Various aryl diazonium salts have been developed utilizing aniline, *para*-substituted (chloro and methyl) aniline, and sulfa drugs as biological counterparts. The previous results of these compounds against RNA coronavirus encouraged the authors to investigate their antiviral activity against DNA viruses, particularly herpes simplex virus type 2. In this study, the authors evaluated the efficacy of 11 newly synthesized pyrimidine derivatives on the viability of Vero cells. The compounds were serially diluted and added to the cell culture, and the cell viability was determined after 72 h via crystal violet assay. The findings showed that most of the new derivatives were not toxic to Vero cells at doses up to 995 micrograms per milliliter (Table 1) Figure 3.

Inhibition mechanisms of action

The evaluation of antiviral activity revealed that compounds 2, 3, and 5c were the most promising new inhibitors of human herpes simplex virus type-2 (HSV-2) among all the tested compounds, which serve as antiviral models for DNA virus inhibition. These compounds demonstrated varying degrees of antiviral activity against HSV-2. The 50% inhibitory concentration (IC_{50}) for these active compounds ranged from 13.9 to 130 $\mu\text{g}/\text{ml}$, as

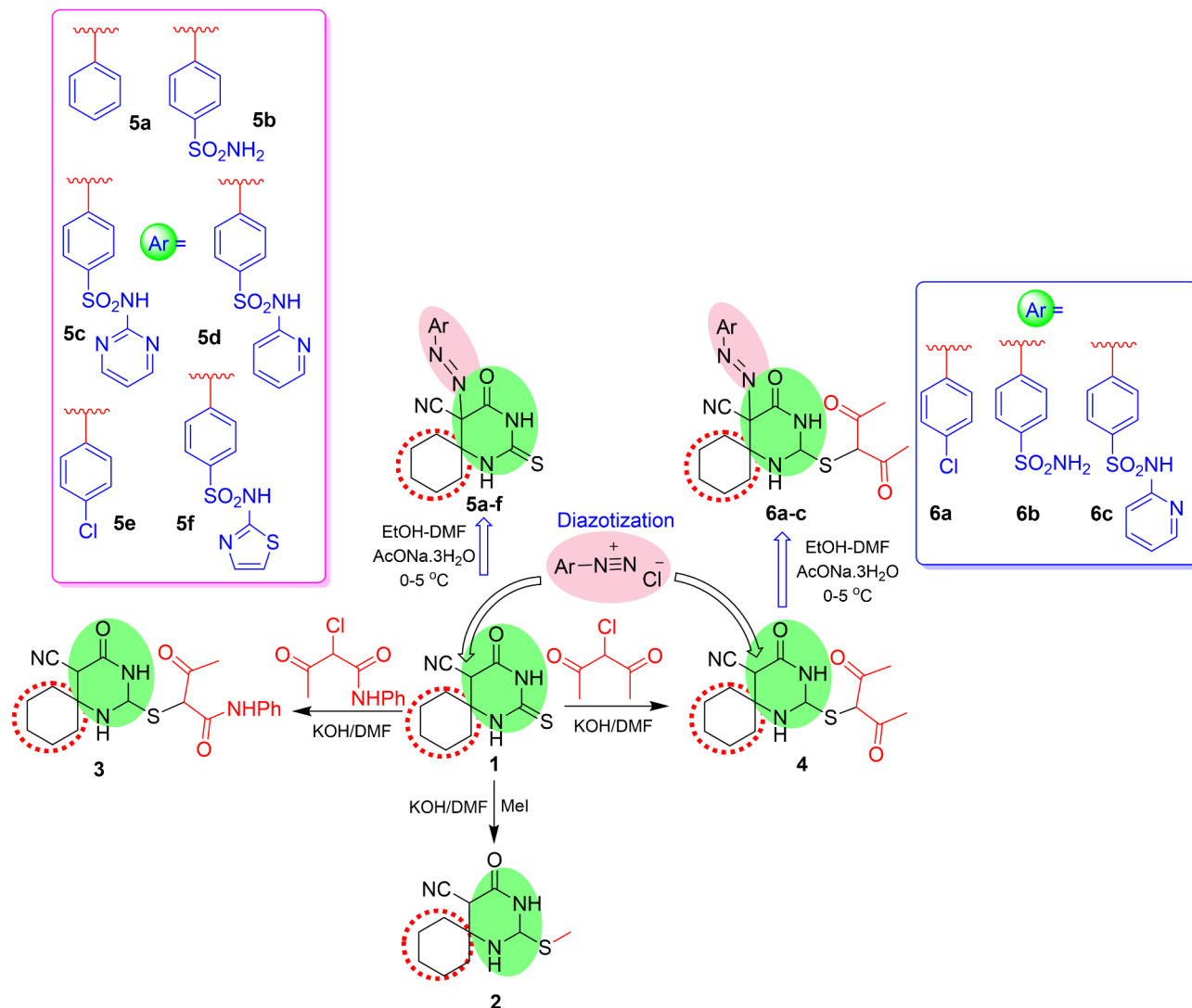


Fig. 2 Synthesis of spirocyclic thiopyrimidinones 2–6

Table 1 Results of the cytotoxicity and inhibitory concentrations of the compounds in various cell lines

Compound	CC ₅₀ (µg/ml)	IC ₅₀ (µg/ml)	SI
2	565.5	130.1	4.34
3	509.30	45.42	11.21
5a	43.89	973.7	0.045
5b	124.3	536.3	0.231
5c	53.66	13.94	3.84
5d	465.5	217.1	2.14
5e	102.6	345.8	0.296
5f	107.0	398.6	0.268
6a	62.39	53.79	1.15
6b	940.1	5406	0.173
6c	42.09	748.8	0.056

detailed in Table 1. Notably, compound 3 effectively suppressed HSV-2 with a favorable selectivity index of 11.2, indicating that it is a strong candidate for further development as an antiviral drug. This study also explored the mechanism of action of these three compounds to gain a deeper understanding of their inhibitory effects on HSV-2. These findings revealed that compound 3 had a significant effect on a crucial stage of the HSV-2 life cycle: viral adsorption. Specifically, 3 resulted in approximately 83% inhibition of HSV-2 adsorption, which is the process through which the virus attaches to and enters host cells. Furthermore, the results indicated that compound 3 also affected another important stage of the HSV-2 life cycle: viral replication, 34% inhibition, and 8% virucidal, where the drug directly affects the viral structure. Next, compound 5c had 42% inhibition of adsorption, 30% replication, and 15% virucidal mechanism. Finally, compound 2 inhibited adsorption by 32%, replication by

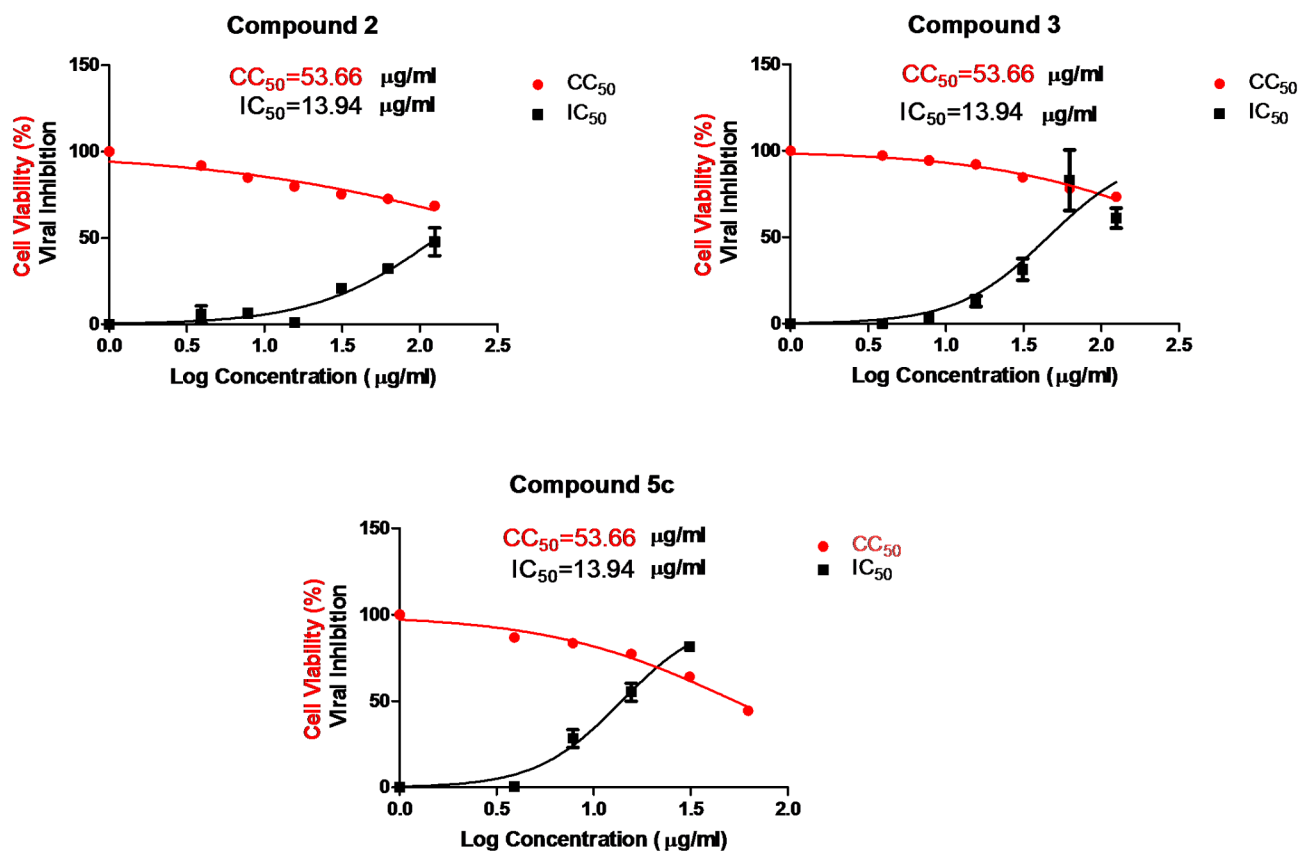


Fig. 3 The plots of the CC_{50} and IC_{50} values are presented in Table 1 for the most promising compounds (2, 3, and 5c)

26%, and the virucidal mechanism by 8%. Importantly, the data showed that the compounds did not influence the virucidal process, indicating that they did not directly inactivate viral particles. (Fig. 4). Additionally, microscopy images revealed the effects of compound 3-induced HSV-2 inhibition through an adsorption mechanism on Vero cells compared with those of the control and control viruses. (Fig. 5)

Western blot

To further validate the impact of promising compounds in mitigating the cellular cytopathic effect (CPE) induced by viral infection, we examined the expression of the caspase-3 protein, which is crucial for the regulation of apoptosis. The objective was to determine whether the reduction in CPE observed with the tested compounds (2, 3, and 5c) was related to alterations in the apoptosis pathway. The results indicated that caspase-3 expression levels, as assessed by Western blotting, decreased at various postinfection time points (1, 3, 6, 12, and 24 h) in the drug-treated viral samples compared with those in the control samples. These findings suggest that the reduction in CPE caused by compound 3 may be specifically associated with its ability to HSV-2 viral infection, hence

downregulating the expression of the caspase-3 protein. (Fig. 6).

Molecular Docking

Finally, docking studies were conducted to investigate the binding mode of compound 3 to the herpes virus entry mediator (HVEM) (PDB ID: 1JMA). The diketone moiety is recognized for its role in enhancing the inhibitory effectiveness of related compounds against various viruses, including the NS2BNS3 proteases of the West Nile virus and the Mayaro virus [25, 26]. In our recent study [24], we reported that incorporating the PhNHOC-CH-COME group into spiropyrimidine compounds led to a twofold increase in their antiviral activity against human coronavirus 229E (HCoV-229E). In the best-ranked binding mode of compound 3, several interactions were observed with the (PhNHOC-CH-COME) group. Hydrogen bonds formed with the side chains of Asn78 and His96, whereas hydrophobic interactions were noted with Val80 via the terminal methyl group of compound 3 and with Asp95 through the phenyl moiety of the compound. Additionally, π - π stacking interactions occurred between the phenyl group of compound 3 and the pyridine ring of His96 (Fig. 7).

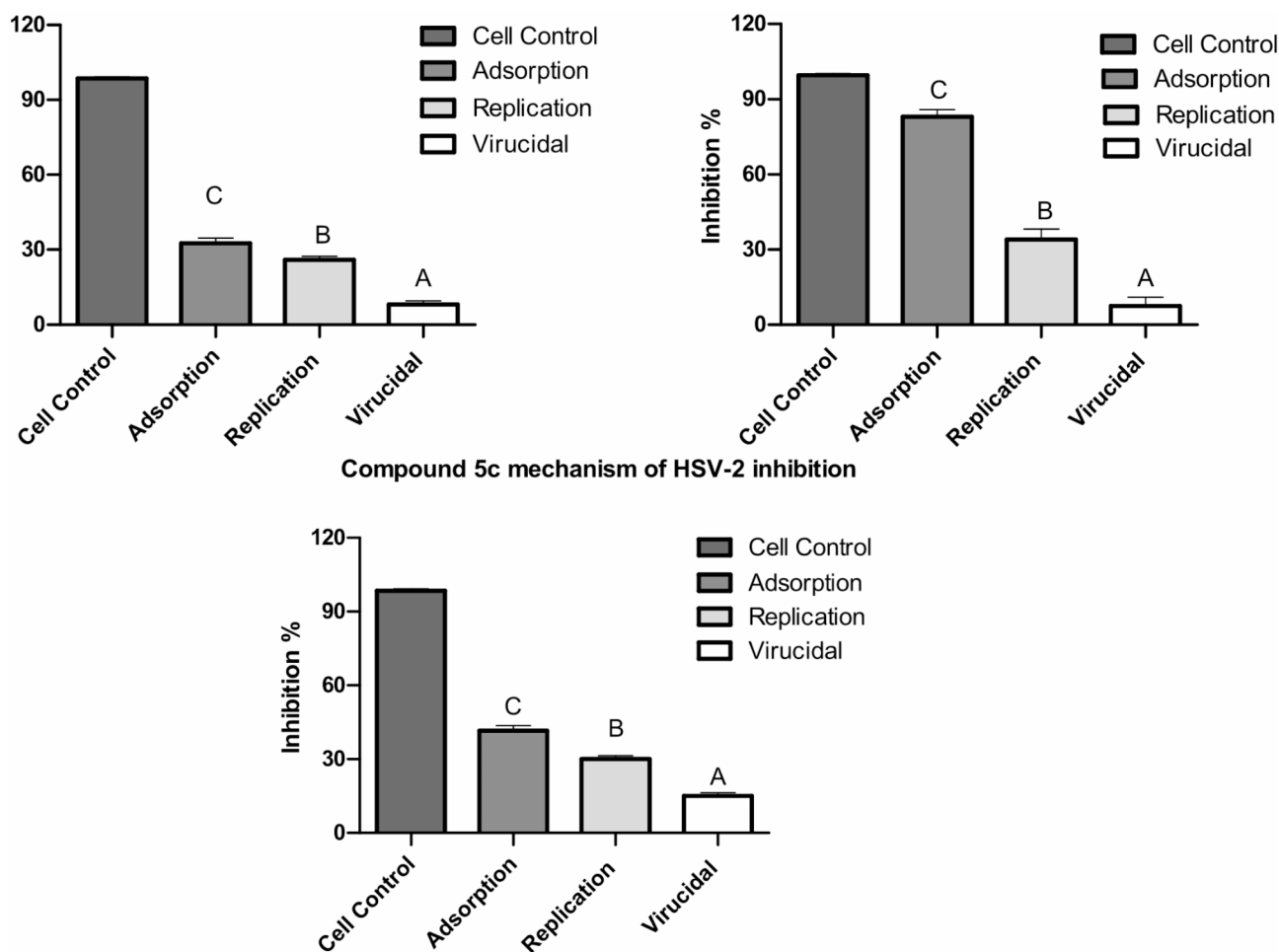


Fig. 4 Mechanism of action of drug candidates 2, 3, and 5c in HSV-2 inhibition. The histograms show the different percentages of HSV-2 inhibition resulting from three different mechanisms of the viral infection life cycle: adsorption, replication, and virucidal. The histogram data are expressed as the mean \pm S.D. of three independent experiments of viral inhibition mechanisms of action against cell control. Groups were statistically analyzed by f tests (ANOVAs) followed by post hoc Duncan tests. Groups with different letters are considered statistically significant at $p < 0.05$

Discussion

Herpes simplex virus (HSV) is a human epidemic that poses a threat to public health. Globally, millions of people are exposed to herpes simplex virus (HSV), with a global seroprevalence of 66% [27], which includes latent infection in neurons, lytic infection of mucosal cells, and reactivation on a regular basis. The advanced immune evasion techniques of HSV lead to several illnesses, such as malignancy, newborn encephalitis, and genital lesions. An efficient preventive or therapeutic vaccination against HSV has not yet been developed, despite more than 70 years of continuous research, mainly because of our limited knowledge of virus–host interactions. The human herpes simplex virus type-2 (HSV-2) is a member of the herpes viral family, which is a group of viruses that infect most people. It is the source of genital herpes, which is the most widespread sexually transmitted disease (STD) worldwide and causes mild to life-threatening infections in humans. It is often an undetected chronic infection

that might increase the prevalence of human immunodeficiency virus (HIV). Antivirals are useful for limiting viral shedding and the duration of symptoms [28–30].

Hence, in this study, we demonstrate a chemical design that synthesizes a novel family of spirocyclic thiopyrimidinone derivatives by integrating several bioactive moieties (pyrimidine, cyano, azo, sulfonamide, diketone, and spirocycles) into a single hybrid. In this context, researchers have mentioned the antiviral effects of one or more members of the same chimeric family on low pathogenic corona virus (229E) [9, 31]. On the basis of these studies, we investigated the compounds' cytotoxicity, antiviral efficacy, and mechanism of action of these new molecules against HSV-2.

At the cytotoxic level, the promising compounds presented various IC_{50} values ranging between 13.94 and 130 $\mu\text{g}/\text{ml}$. While the present data revealed that compound 3 presented the best SI of 11.21, with an IC_{50} of 45.42 $\mu\text{g}/\text{ml}$, compound 2 presented the best IC_{50} of

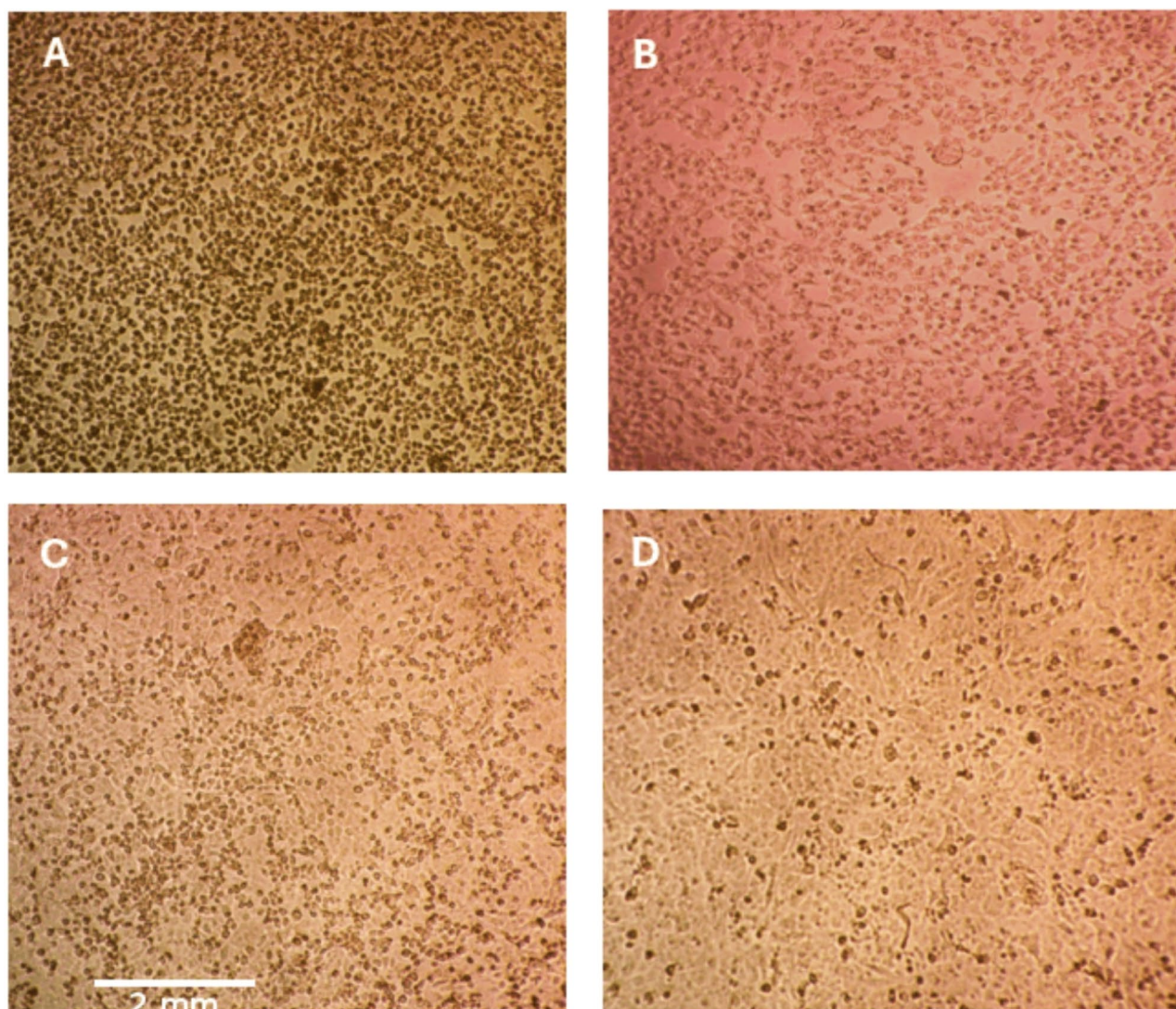


Fig. 5 Microscopy images of the morphological changes in HSV-2-infected Vero cells (MOI=1) treated with compound 3 via different viral infection mechanisms. **A)** Herpes virus control, **B)** infected Vero cells treated with 3 in the replication mechanism, **C)** infected Vero cells treated with 3 in the adsorption mechanism, and **D)** normal Vero cell control

13.94 $\mu\text{g}/\text{ml}$, but its SI was only 4.3, indicating its toxicity to normal cells, with a CC_{50} of 565.5 $\mu\text{g}/\text{ml}$. Thus, compound 3 was selected for all downstream analyses, including an in-depth investigation of the mechanism of action to assess the suitable viral inhibition mechanism, whether it was replication, adsorption or virucidal.

Considering how the antiviral drugs affect HSV-2, compound 3 resulted in 83% viral inhibition by adsorption, 34% by replication, and only 8% by virucidal mechanisms when the host cells were compared with the normal control cells, indicating that adsorption is the major mechanism of viral inhibition for compound 3. While compound 5c showed 42% inhibition by adsorption, 30% inhibition by replication, and 15% inhibition by the virucidal mechanism, and compound 2 had 32% inhibition

by adsorption and 26% inhibition by replication but only 8% inhibition by the virucidal mechanism. Among all the tested compounds, compound 3 is a promising candidate for further research [32].

The antiviral activity of compound 3 could be attributed to its diketone moiety (PhNHOC-CH-COMe), as the ketone group is well known for enhancing the inhibitory efficacy of related compounds against various viruses, including the NS2BNS3 protease of the West Nile virus and the Mayaro virus [26]. Furthermore, in our previous study [24], we reported that incorporating the PhNHOC-CH-COMe group into spiroprymidine compounds resulted in a twofold increase in their antiviral activity against human coronavirus 229E (HCoV-229E).

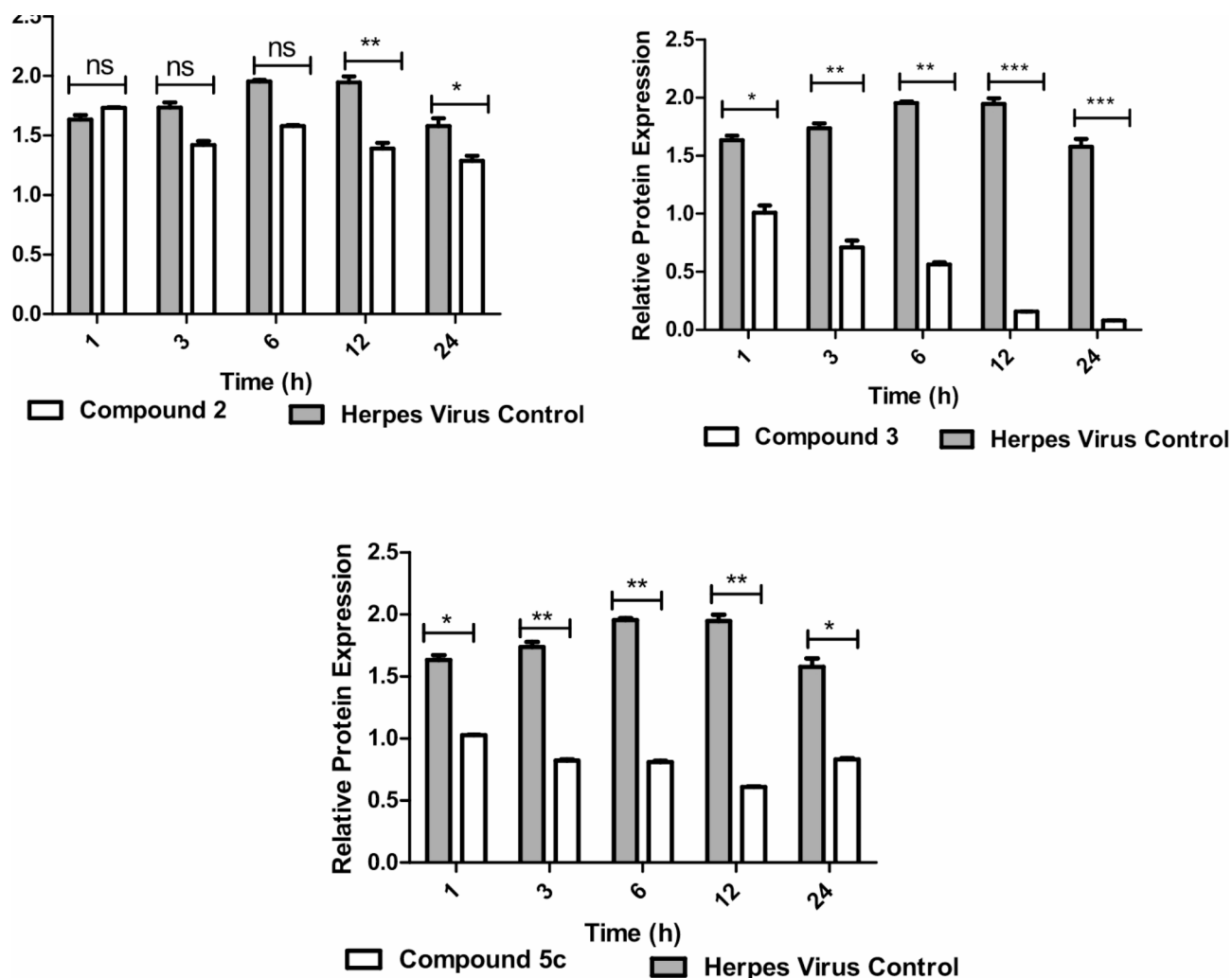


Fig. 6 Western blot analysis for cleaved Caspase-3 protein expression in HSV-2-infected Vero cells (MOI=1) treated with compounds 2, 3, and 5c compared with the HSV-2 virus control (infected Vero cells without any treatment (VC)). **A**) The protein expression level of β -actin at 1 h, 3 h, 6 h, 12 h, and 24 h postinfection. **B**) The protein expression level of Caspase-3 in infected HSV-2 virus control and infected Vero cells treated with 2, 3, or 5c. The measured band intensities of all the compound-treated cells and the virus control were plotted to compare the differences in the protein expression levels of Caspase-3. A *t*-test was used to compare the protein expression levels of caspase-3 in untreated and treated cells. * $p < 0.05$, ** $p < 0.01$, and *** $p < 0.005$. However, ns is not significant

In addition, the newly synthesized compounds resulted in varied levels of cleaved active form Caspase-3 protein expression, as determined by western blotting, compared with the level of expression in Herpes virus control cells. The western blot images revealed a significant decrease in caspase-3 protein levels at 1 h, 3 h, 6 h, 12 h, and 24 h post infection in the 3 treated groups. However, there were slight changes in the expression levels of these genes in the 2- and 5c-treated cells. Therefore, compound 3 inhibited HSV-2 viral infection, as reflected by the gradual downregulation of Caspase-3 protein expression at different time intervals postinfection [33].

In the docking studies of the spirothiopyrimidinone moiety of compound 3, its ketone group-maintained hydrogen bond interactions with the side chain of Asp93

and the backbone amide of Gly94. The nitrogen atoms of the pyrimidine ring also form hydrogen bonds with the side chain of Gln59 and the backbone of His96. Furthermore, hydrophobic interactions with Leu67 were observed. Consequently, the promising inhibitory effect of compound 3 against HSV-2 may be attributed to the interactions of both the spirothiopyrimidinone and (PhNHOC-CH-COMe) moieties within the binding pocket of HVEM, which differs from that of HSV-2. These findings suggest that compound 3 functions as an entry inhibitor by allosterically interacting with HVEM, altering its conformation and ultimately affecting HSV-2 virus adsorption [34].

Eventually, this study successfully identified compound 3 (2-((5-cyano-4-oxo-1,3-diazaspiro[5.5]undecan-2-yl)

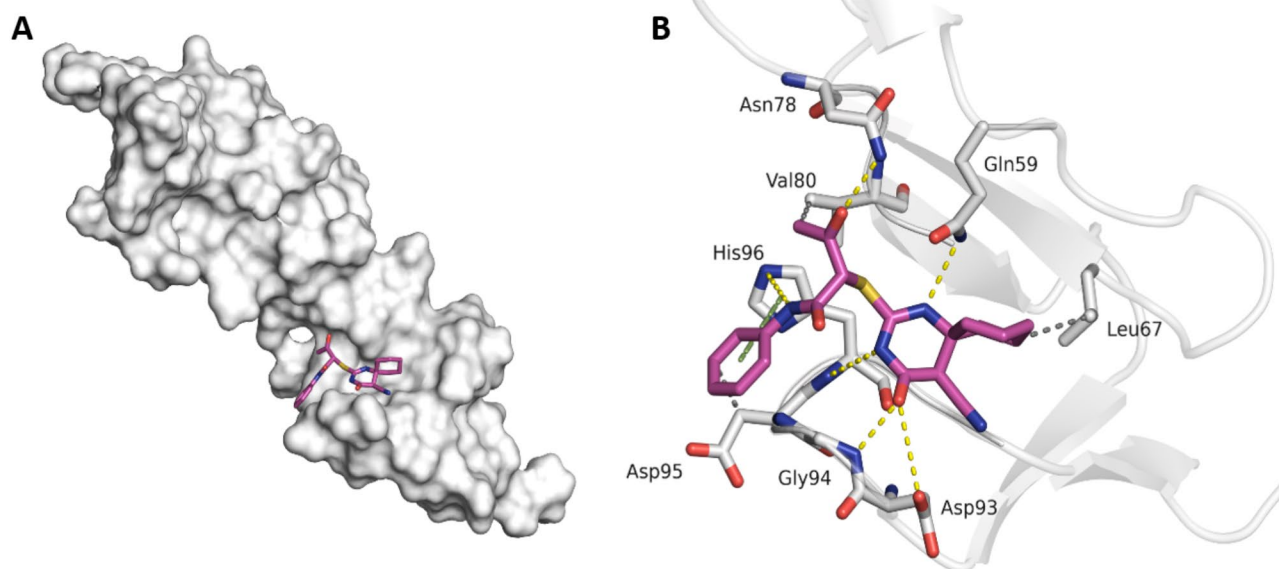


Fig. 7 **A**) The best ranked binding mode of 3 in HVEM. **B**) The best ranked binding mode of 3 (magenta) in the binding pocket of HVEM (PDB ID 1JMA). Hydrogen bonding interactions, hydrophobic interactions and π - π interactions are colored yellow, gray, and green, respectively

thio)-3-oxo-N-phenylbutanamide) as a potent inhibitor of HSV-2, contributing to the ongoing search for effective antiviral therapies against herpesvirus type 2 (HSV-2). These findings demonstrate that compound 3 interferes with critical stages of the HSV-2 life cycle, viral adsorption and replication while also exhibiting a favorable selectivity index and minimal cytotoxicity to normal cells. The association between the structure of 3, particularly its diketone moiety, and its antiviral activity underscores the potential for developing new antiviral agents on the basis of similar chemical frameworks. These docking studies provide insights into the binding interactions of compound 3 with HVEM, suggesting a novel mechanism of action as an entry inhibitor. Overall, these results pave the way for further investigation and optimization of this structural formula of compound 3 and its derivatives as viable therapeutic options for HSV-2 infections.

Abbreviations

HSV-2	Herpes Simplex Virus type 2
HIV	Human Immunodeficiency Virus
STDs	Sexually transmitted diseases
CPE	Cytopathic effect
FBS	Fetal bovine serum
BSA	Bovine serum albumin
DMEM	Dulbecco's modified Eagle medium
PBS	Phosphate buffered saline
DMSO	Dimethyl sulfoxide
MTT	(3-(4, 5-dimethylthiazolyl)-2, 5-diphenyltetrazolium bromide) assay
CC50	Half maximal cytotoxicity concentration
IC50	Half maximal inhibitory concentration
SI	Selective index
VC	Virus control
CC	Cell Control
SDS-PAGE	Sodium dodecyl-sulfate polyacrylamide gel electrophoresis
RIPA buffer	Radioimmunoprecipitation assay buffer
PVDF membrane	Polyvinylidene difluoride

HVEM

Herpes Virus Entry Mediator

Acknowledgements

I would like to thank Seif Ehab for his advice and suggestions in this article. They were vital in inspiring me to think outside the box, from multiple perspectives to form a comprehensive and objective critique.

Author contributions

E.A.M.: contribution to the conception and design of the work; interpretation of data; wrote the first draft of manuscript text; E.M.E.: contribution to the conception and design of the work; drafted the work and substantively revised it; S.S.R.: prepared figures and tables; chemical synthesis preparations; A.M.S.: prepared figures and tables; chemical synthesis preparations; H.I.: review the first draft; interpretation of data; S.N.: Molecular Docking; prepared figures and tables; A.K.A.: contribution to the conception and design of the work; revised the main manuscript text.

Funding

Open access funding provided by The Science, Technology & Innovation Funding Authority (STDF) in cooperation with The Egyptian Knowledge Bank (EKB).

There is no funding source for this study.

Data availability

No datasets were generated or analysed during the current study.

Declarations

Ethics approval and consent to participate

Not applicable.

Consent for publication

We hereby grant our consent for the publication of our manuscript and confirm that all coauthors have agreed to this submission.

Competing interests

The authors declare no competing interests.

Author details

¹Biotechnology Program, Faculty of Science, Cairo University, Dokki, Giza, Egypt

²Department of Biotechnology, Faculty of Science, Cairo University, Dokki, Giza, Egypt

³Photochemistry Department, Chemical Industries Research Institute, National Research Centre (NRC), 33 El-Behouth St., Dokki, Giza 12622, Egypt

⁴Department of the Chemistry of Natural and Microbial Products, Pharmaceutical and Drug Industries Institute, National Research Centre (NRC), 33 El-Behouth St., Dokki, Giza 12622, Egypt

⁵Chemistry Department, Faculty of Science, Cairo University, Dokki, Giza, Egypt

⁶Department of Pharmaceutical Chemistry, Faculty of Pharmacy and Biotechnology, German University in Cairo, New Cairo City, Cairo 11835, Egypt

⁷Virology Lab, Water Pollution Research Department, Environment and Climate Change Institute, National Research Centre, Dokki, Giza 12622, Egypt

Received: 3 February 2025 / Accepted: 13 March 2025

Published online: 11 April 2025

References

- Vaslin MFS, Arruda LB, Campos FS, Surveillance. Prevention, evolution and control of emerging viruses: A 2022 editorial update. *Viruses*. 2023;15(10):2098. <https://doi.org/10.3390/v15102098>.
- Kausar S, Said Khan F, Ishaq Muejeb Ur Rehman M, Akram M, Riaz M, Rasool G, Hamid Khan A, Saleem I, Shamim S, Malik A. A review: mechanism of action of antiviral drugs. *Int J Immunopathol Pharmacol* 2021 Jan-Dec;35:20587384211002621. <https://doi.org/10.1177/20587384211002621>
- Spear PG, Longnecker R. Herpesvirus entry: an update. *J Virol*. 2003;77(19):10179–85. <https://doi.org/10.1128/jvi.77.19.10179-10185.2003>. <https://www.who.int/news-room/fact-sheets/detail/herpes-simplex-virus>
- Ostlund EN. The equine herpesviruses. *Vet Clin North Am Equine Pract*. 1993;9(2):283–94. [https://doi.org/10.1016/s0749-0739\(17\)30396-6](https://doi.org/10.1016/s0749-0739(17)30396-6).
- Omarova S, Cannon A, Weiss W, Bruccoleri A, Puccio J. Genital herpes simplex Virus-An updated review. *Adv Pediatr*. 2022;69(1):149–62. <https://doi.org/10.1016/j.yapd.2022.03.010>.
- Simmons A. Clinical manifestations and treatment considerations of herpes simplex virus infection. *J Infect Dis*. 2002;186(Suppl 1):S71–7. <https://doi.org/10.1086/342967>.
- Zhu S, Viejo-Borbolla A. Pathogenesis and virulence of herpes simplex virus. *Virulence*. 2021;12(1):2670–702. <https://doi.org/10.1080/21505594.2021.1982373>.
- Ragab SS, Sweed AM, Hamza ZK, Shaban E, El-Sayed AA, Design. Synthesis, and antibacterial activity of spiropyrimidinone derivatives incorporated Azo sulfonamide chromophore for polyester printing application. *Fib Polym*. 2022;23:2114–22. <https://doi.org/10.1007/s12221-022-4032-4>.
- Allayeh AK, El-boghdady AH, Said MA, Saleh MGA, Abdel-Aal MT, Abouele-nein MG. Discovery of Pyrano[2,3-c] pyrazole derivatives as novel potential human coronavirus inhibitors: design, synthesis, in Silico, in vitro, and ADME studies. *Pharmaceuticals*. 2024;17(198). <https://doi.org/10.3390/ph17020198>.
- Rasha Z, Batran; Ahmed S, Mohammed A, Khedr; Abdou K, Allayeh. Christophe Pannecouque; Asmaa F. Kassem; 4-Phenylcoumarin derivatives as new HIV-1 NNRTIs: design, synthesis, biological activities, and computational studies. *Bioorg Chem*. 2023;141:106918.
- Hend Hekal O, Hammad N, El-Brollosy M, Salem AK, Allayeh. Design, synthesis, docking, and antiviral evaluation of some novel pyrimidinone-based α -aminophosphonates as potent H1N1 and HCoV-229E inhibitors. *Bioorg Chem*. 2024;147:107353.
- Carfi A, Willis SH, Whitbeck JC, Krummenacher C, Cohen GH, Eisenberg RJ, Wiley DC. Herpes simplex virus glycoprotein D bound to the human receptor HveA. *Mol Cell*. 2001;8(1):169–79.
- Jo S, Kim T, Iyer VG, Im W. CHARMM-GUI: A Web-based graphical user interface for CHARMM. *J Comput Chem*. 2008;29:1859–65.
- Jo S, Cheng X, Islam SM, Huang L, Rui H, Zhu A, Lee HS, Qi Y, Han W, Vanommeslaeghe K, Mackerell AD Jr., Roux B, Im W. CHARMM-GUI PDB manipulator for advanced modeling and simulations of proteins containing nonstandard residues. *Adv Protein Chem Struct Biol*. 2014;96:235–65.
- S.J. Park, N.R. Kern, T. Brown, J. Lee, and W. Im (2023) CHARMM-GUI PDB Manipulator: Various PDB Structural Modifications for Biomolecular Modeling and Simulation (2023) *J. Mol. Biol.* 167995
- UCSF Chimera—a visualization system for exploratory research and analysis, Pettersen EF, Goddard TD, Huang CC, Couch GS, Greenblatt DM, Meng EC, Ferrin TE. *J Comput Chem*. 2004;25(13):1605–12.
- Guilloux VL, Schmidtke P, Tuffery P. Fpocket: an open-source platform for ligand pocket detection. *BMC Bioinformatics*. 2009;10:168.
- Tian et al. *Nucleic Acids Res*. 2018. PMID: 29860391 <https://doi.org/10.1093/nar/gky473>
- Jones G, Willett P, Glen RC. Molecular recognition of receptor sites using a genetic algorithm with a description of desolvation. *J Mol Biol*. 1995;245(1):43–53. <https://doi.org/10.1016/S0022->
- Jones G, Willett P, Glen RC, Leach AR, Taylor R. Development and validation of a genetic algorithm for flexible Docking. *J Mol Biol*. 1997;267(3):727–48. <https://doi.org/10.1006/jmbi.1996.0897>.
- Adasme MF, et al. PLIP 2021: expanding the scope of the protein–ligand interaction profiler to DNA and RNA. *Nucl Acids Res* (2 July. 2021;49(W1):W530–4. <https://doi.org/10.1093/nar/gkab294>.
- The PyMOL Molecular. Graphics System, Version 2.5.4 Schrödinger, LLC.
- Ragab SS, Sweed AMK, Elrashedy AA, Allayeh AK, Design. Synthesis, Antiviral Evaluation, and Molecular Dynamics Simulation Studies of New Spirocyclic Thiopyrimidinones as Anti HCoV-229E. *Chem. Biodivers*. 19 (2022) e202200632. Doi.10.1002/cbdv.202200632.
- Gazolla P, Oliveira A, Pereira W, Maia A, Santos E, Mendes T, Dias R, Polêto M, Teixeira R. Discovery of novel West Nile virus protease inhibitor based on isobenzonafuranone and triazolol derivatives of Eugenol and indan-1,3-dione scaffolds. *PLoS ONE*. 2019;14:e0223017–0223017.
- Fernandes LS, da Silva ML, Dias RS, da S Lucindo MS, da Silva ÉE, Silva CC, Teixeira RR, de Paula SO. Evaluation of antiviral activity of cyclic ketones against Mayaro virus. *Viruses*. 2021;13:2123–34.
- Rebecca I, Montgomery · Morgyn S, Warner · Brian J. Lum · Patricia G spear, herpes simplex Virus-1 entry into cells mediated by a novel member of the TNF/NGF receptor family. 87, Issue 3 P427–36 1996 Open Archive.
- Poole CL, James SH. Antiviral therapies for herpesviruses: current agents and new directions. *Clin Ther*. 2018;40(8):1282–98. <https://doi.org/10.1016/j.clinthera.2018.07.006>. Epub 2018 Aug 10. PMID: 30104016; PMCID: PMC7728158.
- Helen O, Edogbanya SO, Momoh U, Sani. Herpes simplex virus type–2 (HSV-2) and HIV coinfection dynamics with optimal control. *Int J Dev Math* 2024. 2024;1(1). <https://doi.org/10.62054/ijdm/0101.09>.
- Bai L, Xu J, Zeng L, et al. A review of HSV pathogenesis, vaccine development, and advanced applications. *Mol Biomed*. 2024;5:35. <https://doi.org/10.1186/s43556-024-00199-7>.
- Ragab SS, Ibrahim NE, Abdel-Aziz MS, Elrashedy AA, Allayeh AK. Synthesis, biological activity, and molecular dynamic studies of new Triazolopyrimidine derivatives. *Results Chem*. 2023;6:101163. <https://doi.org/10.1016/j.rechem.2023.101163>.
- Lycke E, Johansson M, Svennerholm B, et al. Binding of herpes simplex virus to cellular Heparan sulphate, an initial step in the adsorption process. *J Gen Virol*. 1991;72(Pt 5):1131–7.
- Li L, Kovacs SB, Jørgensen I, Larson HN, Lazear HM, Miao EA. Role of caspases and gasdermin A during HSV-1 infection in mice. *Viruses*. 2022;14(9):2034. <https://doi.org/10.3390/v14092034>.
- Madavaraju K, Koganti R, Volety I, Yadavalli T, Shukla D. Herpes simplex virus cell entry mechanisms: an update. *Front Cell Infect Microbiol*. 2021;10:617578. <https://doi.org/10.3389/fcimb.2020.617578>.

Publisher's note

Springer Nature remains neutral with regard to jurisdictional claims in published maps and institutional affiliations.